Proceedings of 2016 IEEE
International Conference on Mechatronics and Automation
August 7 - 10, Harbin, China

Time-varying Spectrum Based Active Disturbance Rejection Control for Hypersonic Reentry Vehicle

Zhiqiang Pu[1], Jianhong Zhang[2], Ruyi Yuan[1], and Jianqiang Yi[1]

[1] *Institute of Automation, Chinese Academy of Sciences*
Beijing, 100190,China
{zhiqiang.pu & ruyi.yuan & jianqiang.yi}@ia.ac.cn

[2] *Beijing Aerospace Automatic Control Institute*
Beijing, 100854 China
zhangjianhong167@163.com

***Abstract* –This paper proposes a robust attitude control strategy for hypersonic reentry vehicles which combines novel time-varying spectrum based active disturbance rejection control techniques with a basic stabilizing controller. These techniques include time-varying tracking differentiator (TTD) and time-varying extended state observer (TESO). By adopting time-varying bandwidth, TTD can adaptively arrange transient processes for either abrupt or smooth reference commands. Also by designing time-varying bandwidth logic, TESO can not only estimate total disturbance well, but also suppress peaking phenomenon resulting from initial reentry condition dispersion. Several simulations are conducted which demonstrate that the proposed control strategy exhibits both good attitude tracking ability and great design flexibility.**

Index Terms – Hypersonic Vehicle, Reentry, Active Disturbance Rejection Control, Time-varying Spectrum

I. INTRODUCTION

With rapid development of next generation of reusable launch vehicles, design of robust reentry attitude control systems that meet safety, reliability, and low-cost requirements has drawn more and more attention in these decades [1][2]. Reentry flight has to operate over a large flight envelope within which diverse uncertainties exist inevitably. Particularly, transition from cruise to entry flight may undergo large initial transition condition dispersion. In addition, entry flight usually involves super maneuvers with diverse command shapes but constrained actuator torques. All these factors make hypersonic reentry attitude control a difficult and challenging task.

A conventional approach to entry control is gain scheduling (GS) [3]. However, due to large flight envelope and fast time-varying feature, GS control design is time-consuming and requires solid engineering experience. Hence, advanced nonlinear control methods have been developed for the last few decades. Feedback linearization has been widely applied as a basic tool. In [2], it was combined with a model predictive method to solve the constrained input and state problem. An adaptive control strategy was developed in [4] where back-stepping approach was applied to decompose the whole system into several subsystems. Trajectory linearization control system was designed in [5] where the plant was linearized near nominal trajectories and control system was developed using LTV spectrum theories. Similar idea was presented in [6], but dynamic inversion rather than LTV spectrum method was then integrated to stabilize the closed-loop system.

As an alternative, active disturbance rejection control (ADRC) [7][8][9][10] has been well developed with simple structure and satisfactory disturbance rejection performance. ADRC lumps both internal and external disturbances together as an extended state and estimates this state by using a unique extended state observer (ESO). ADRC also arranges proper transient process for a given reference command according to system control ability by using a tracking differentiator (TD), which helps to solve the conflict between fast response and overshoot.

Conventional ADRC chooses either linear (time-invariant) or nonlinear structures to design ESO. However, both have inherent drawbacks: linear approach has less design flexibility and performs worse especially in complex systems; nonlinear structures make theoretical derivation for ADRC much more difficult. For these problems, in our previous work [9], a novel adaptive ESO was proposed where the observer gains were designed in a linear time-varying form and time-varying PD spectrum theories were adopted to analyze convergence and observation error bound of the observer. In this paper, this time-varying spectrum idea is adopted and expanded to design both time-varying ESO (TESO) and time-varying TD (TTD) for hypersonic attitude system. Our purpose is to solve the following three issues. Particularly, the last two issues have received far insufficient attention in current researches.

- *Disturbance rejection*. For both internal and external disturbances, TESO is designed for robust disturbance estimation and compensation.
- *Initial transition condition dispersion*. Large observer gains can improve the performance of ESO. But high gains may also cause peaking phenomenon due to initial condition dispersion during the transition from cruise to entry flight. A specific time-varying discipline for the TESO is designed to solve this conflict.
- *Adaptive reference command shaping*. As discussed before, entry flight often involves large maneuvers with diverse command forms (sine, square, etc.). Due to constrained control torques, the vehicle exhibits quite different tracking abilities for different reference commands. TTD is designed as an adaptive command shaping filter to solve this problem.

II. MODEL DESCRIPTION

In this paper, a winged-cone configuration generic hypersonic vehicle (GHV) [11] is researched. During its entry flight, the engine is shut down and the configured canards are disabled. Since it is equipped with no reaction-control system, GHV will be controlled only by the aerodynamic-control surfaces: two trailing edge elevons (deflection angles δ_a

and δ_e, positive up) and a full span rudder (deflection angle δ_r, positive left) . The attitude dynamics of this unpowered vehicle with disturbances can be described as [12]:

$$\dot{\alpha} = q - \tan\beta(p\cos\alpha + r\sin\alpha) + \frac{-L + mg\cos\gamma\cos\mu}{mV\cos\beta} + \Delta_1 \quad (1)$$

$$\dot{\beta} = p\sin\alpha - r\cos\alpha + \frac{Y\cos\beta + mg\cos\gamma\sin\mu}{mV} + \Delta_2 \quad (2)$$

$$\dot{\mu} = \frac{p\cos\alpha + r\sin\alpha}{\cos\beta} + \frac{1}{mV}(L\tan\gamma\sin\mu + L\tan\beta + Y\tan\gamma\cos\mu\cos\beta - mg\cos\gamma\cos\mu\tan\beta) + \Delta_3 \quad (3)$$

$$\dot{p} = \left[\bar{L} + (I_y - I_z)qr\right]/I_x + \Delta_4 \quad (4)$$

$$\dot{q} = \left[\bar{M} + (I_z - I_x)pr\right]/I_y + \Delta_5 \quad (5)$$

$$\dot{r} = \left[\bar{N} + (I_x - I_y)pq\right]/I_z + \Delta_6 \quad (6)$$

Δ_j, $j = 1 \sim 6$, represents total disturbance in each channel, including internal structural and parametric uncertainties, and external disturbances. Equations (1)-(3) govern the attitude angles where α, β, and μ are the angle of attack, sideslip angle, and bank angle. Equations (4)-(6) govern the body-axis rates where p, q, and r are the roll, pitch, and yaw rates respectively. m, g, V are the vehicle mass, gravity constant, and velocity. I_x, I_y, I_z are moments of inertia. The lift L, side force Y, and body torques $\bar{L}$, $\bar{M}$, $\bar{N}$ are expressed as:

$$\begin{cases} L = \bar{q}S_{ref}[C_L(Ma,\alpha) + C_{L2}(\delta_a,\delta_e)] \\ Y = \bar{q}S_{ref}[C_Y(Ma,\alpha,\beta) + C_{Y2}(\delta_a,\delta_e,\delta_r)] \end{cases} \quad (7)$$

$$\begin{cases} \bar{L} = \bar{q}bS_{ref}C_{\bar{L}}(Ma,\alpha,\beta,\delta_a,\delta_e,\delta_r) \\ \bar{M} = \bar{q}cS_{ref}C_{\bar{M}}(Ma,\alpha,\beta,\delta_a,\delta_e,\delta_r) \\ \bar{N} = \bar{q}bS_{ref}C_{\bar{N}}(Ma,\alpha,\beta,\delta_a,\delta_e,\delta_r) \end{cases} \quad (8)$$

where $\bar{q} = 0.5\rho V^2$ is the dynamic pressure with ρ as air density. S_{ref}, b, c are the reference area, lateral reference length, and mean aerodynamic chord, respectively, and Ma is the Mach number. To describe a high-fidelity aerodynamic model covering whole entry flight envelope, the aerodynamic coefficients are fitted as high-order polynomials with respect to relevant flight states and deflection angles [11]. This high-fidelity model presents sever nonlinear, fast time-varying, and significant couplings characteristics, which pose huge challenges to robust control design.

For control design purpose, simplification is made to the aerodynamic model (7)-(8). First, it is verified that the aerodynamic forces generated by deflections are negligible, thus (7) is simplified as

$$\begin{cases} L = \bar{q}S_{ref}C_L(Ma,\alpha) \\ Y = \bar{q}S_{ref}C_Y(Ma,\alpha,\beta) \end{cases} \quad (9)$$

where the neglected items can be lumped into $\Delta_1 \sim \Delta_3$. Second, first-order Taylor expansion is applied to the torques for producing their approximate linear forms with respect to the deflections [12]:

$$\begin{cases} \bar{L} = \bar{L}_0 + L_a\delta_a + L_e\delta_e + L_r\delta_r \\ \bar{M} = \bar{M}_0 + M_a\delta_a + M_e\delta_e + M_r\delta_r \\ \bar{N} = \bar{N}_0 + N_a\delta_a + N_e\delta_e + N_r\delta_r \end{cases} \quad (10)$$

where $\bar{L}_0$, $\bar{M}_0$, $\bar{N}_0$ are independent of the deflections. High-order approximation errors can be lumped into the total disturbances $\Delta_4 \sim \Delta_6$.

In addition, the control surfaces are modelled as first-order low-pass filters with certain gains. Limits on deflection and rate are separately set as:

$$-30^\circ \le \delta_a, \delta_e, \delta_r \le 30^\circ \quad (11)$$

$$-180^\circ \cdot \sec^{-1} \le \dot{\delta}_a, \dot{\delta}_e, \dot{\delta}_r \le 180^\circ \cdot \sec^{-1} \quad (12)$$

Redefine

$$X_1 = \begin{bmatrix} \alpha \\ \beta \\ \mu \end{bmatrix},\ X_2 = \begin{bmatrix} p \\ q \\ r \end{bmatrix},\ U = \begin{bmatrix} \delta_a \\ \delta_e \\ \delta_r \end{bmatrix},\ \Delta_s = \begin{bmatrix} \Delta_1 \\ \Delta_2 \\ \Delta_3 \end{bmatrix},\ \Delta_f = \begin{bmatrix} \Delta_4 \\ \Delta_5 \\ \Delta_6 \end{bmatrix}$$

The subscripts s and f denote slow-state loop (attitude) and fast-state loop (angular rate) respectively. The hypersonic model (1)-(6), (9) -(10) can be written in a concise form as

$$\dot{X}_1 = F_1(X_1) + G_1(X_1)X_2 + \Delta_s \quad (13)$$

$$\dot{X}_2 = F_2(X_1, X_2) + G_2(X_1)U + \Delta_f \quad (14)$$

where

$$F_1 = \begin{bmatrix} (-L + mg\cos\gamma\cos\mu)/(mV\cos\beta) \\ (Y\cos\beta + mg\cos\gamma\sin\mu)/(mV) \\ (L\tan\gamma\sin\mu + L\tan\beta + Y\tan\gamma\cos\mu\cos\beta - mg\cos\gamma\cos\mu\tan\beta)/(mV) \end{bmatrix}$$

$$G_1 = \begin{bmatrix} -\cos\alpha\tan\beta & 1 & -\sin\alpha\tan\beta \\ \sin\alpha & 0 & -\cos\alpha \\ \cos\alpha\sec\beta & 0 & \sin\alpha\sec\beta \end{bmatrix}$$

$$F_2 = \begin{bmatrix} [\bar{L}_0 + (I_y - I_z)qr]/I_x \\ [\bar{M}_0 + (I_z - I_x)pr]/I_y \\ [\bar{N}_0 + (I_x - I_y)pq]/I_z \end{bmatrix} \quad G_2 = \begin{bmatrix} L_a & L_e & L_r \\ M_a & M_e & M_r \\ N_a & N_e & N_r \end{bmatrix}$$

III. Robust Attitude Control Design

In this section, we will design a robust control scheme for the hypersonic attitude system (13)-(14). This scheme combines a basic dynamic inversion strategy and two time-varying spectrum based ADRC techniques, i.e., TESO and TTD. The dynamic inversion builds a basic stabilizing control law, while TESO and TTD are integrated to improve system robustness in the presence of multi-sources disturbances, large initial transition condition dispersion, and diverse reference commands. As (13)-(14) construct a cascade system where both attitude and angular rate subsystems have similar internal structures, the control scheme mentioned above is similarly adopted in these two subsystems. The overall control scheme is illustrated as Fig. 1.

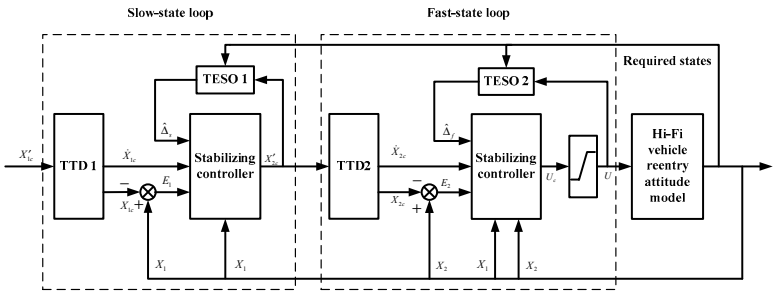

Fig.1 Overall control scheme.

Next we separately address the design of basic dynamic inversion control law, TESO, and TTD.

A. Basic dynamic inversion control design

In basic control law design, disturbances are neglected. For undisturbed system (13), assume $G_1(X_1)$ is nonsingular, which is verified to be admissible in the whole flight envelope. Then selecting a control law

$$X_2 = G_1^{-1}(X_1)[U_1 - F_1(X_1)] \tag{15}$$

leaves the slow-state loop in the integrator-decoupled form

$$\dot{X}_1 = U_1 \tag{16}$$

where U_1 is a virtual control variable. Denote the reference attitude angle and its derivative as X_{1c} and $\dot{X}_{1c}$ which are generated by original attitude command X'_{1c} using TTD (addressed later). Define attitude tracking error as $E_1 = X_1 - X_{1c}$, then

$$\dot{E}_1 = U_1 - \dot{X}_{1c} \tag{17}$$

Selecting the virtual control $U_1 = -K_1 E_1 + \dot{X}_{1c}$ yields

$$\dot{E}_1 = -K_1 E_1 \tag{18}$$

where K_1 is the control gain to be tuned. Choosing $K_1 > 0$ can guaranteed the closed-loop stability. Take U_1 back into (15), and denote the control variable X_2 as X'_{2c}, which means it is the reference command for subsequent angular rate subsystem. The basic dynamic inversion control law for the slow-state loop is

$$X'_{2c} = G_1^{-1}(X_1)[-K_1 E_1 + \dot{X}_{1c} - F_1(X_1)] \tag{19}$$

B. Time-varying extended state observer design

The basic control law (19) is designed for the undisturbed vehicle dynamics. When diverse uncertainties and disturbances are considered, the control performance may be significantly degraded. For this issue, a TESO is constructed for uncertainty estimation and compensation. Consider the disturbed slow-state dynamics (13), where Δ_s contains total disturbance. Define $\dot{\Delta}_s = H_s$, $H_s = [h_\alpha \; h_\beta \; h_\mu]^T$, with the assumption that H_s is unknown but bounded. Redefine $X_{s1} = X_1$, $X_{s2} = \Delta_s$, where the total disturbance is taken as an extended state. Then (13) can be written into an extended system:

$$\begin{cases} \dot{X}_{s1} = F_1(X_{s1}) + G_1(X_{s1})X_2 + X_{s2} \\ \dot{X}_{s2} = H_s \end{cases} \tag{20}$$

For this system, following our previous work [9], a TESO is designed as

$$\begin{cases} \dot{Z}_1 = F_1(X_{s1}) + G_1(X_{s1})X_2 + Z_2 - L_1(t)\tilde{E}_1 \\ \dot{Z}_2 = -L_2(t)\tilde{E}_1 \end{cases} \tag{21}$$

where

$$L_1(t)=\text{diag}\{l_{1\alpha}(t), l_{1\beta}(t), l_{1\mu}(t)\}$$
$$L_2(t)=\text{diag}\{l_{2\alpha}(t), l_{2\beta}(t), l_{2\mu}(t)\}$$

Here Z_1 and Z_2 are the estimated values of the state X_{s1} and the total disturbance X_{s2}, and $\tilde{E}_1 = Z_1 - X_{s1}$ is the estimation error of X_{s1}. Compared with conventional linear or nonlinear ESO, the novelty of TESO lies in that it utilizes linear time-varying gains $L_1(t)$ and $L_2(t)$, rather than LTI or nonlinear structures, to construct the observer. This time-varying mechanism offers better flexibility for performance enhancement (compared with linear ESO) and much simpler structure for theoretical derivation (compared with nonlinear ESO).

Equation (21) minus (20) produces estimation error dynamics for the three attitude angles as follow:

$$\dot{\tilde{e}}_i = A_i(t)\tilde{e}_i + b_i(-h_i) \tag{22}$$

where

$$\tilde{e}_i = \begin{bmatrix} \tilde{e}_{1i} \\ \tilde{e}_{2i} \end{bmatrix},\; A_i(t) = \begin{bmatrix} -l_{1i}(t) & 1 \\ -l_{2i}(t) & 0 \end{bmatrix},\; b_i = \begin{bmatrix} 0 \\ 1 \end{bmatrix},\; i = \alpha, \beta, \mu$$

and $\tilde{e}_{1i}, \tilde{e}_{2i}$ are estimation errors of corresponding attitude angle and total disturbance. For this LTV system (22), TESO utilizes differential algebraic spectral theory for assigning proper time-varying PD-spectrum to guarantee convergence of the observer. For this second-order TESO, assign its PD-spectrum as [9]

$$\rho_{1i}(t), \rho_{2i}(t) = \begin{cases} -\zeta_i \omega_{ni}(t) \pm j\omega_{ni}(t)\sqrt{1-\zeta_i^2}, & 0 < |\zeta_i| < 1 \\ -\omega_{ni}(t), -\omega_{ni}(t) + \omega_{ni}(t) / \int \omega_{ni}(t)dt, & |\zeta_i| = 1 \\ -(\zeta_i \pm \sqrt{\zeta_i^2 - 1})\omega_{ni}(t), & |\zeta_i| > 1 \end{cases} \tag{23}$$

where ζ_i is a constant damping ratio, $\omega_{ni}(t)$ is the assigned time-varying observer bandwidth. Similar to the pole assignment method for LTI system, the observer gains $l_{1i}(t)$, $l_{2i}(t)$ can be expressed through the PD-spectrum as

$$\begin{cases} l_{1i}(t) = 2\zeta_i \omega_{ni}(t) - \dot{\omega}_{ni}(t) / \omega_{ni}(t) \\ l_{2i}(t) = \omega_{ni}^2(t) + \ddot{\omega}_{ni}(t) / \omega_{ni}(t) - 2\zeta_i \dot{\omega}_{ni}(t) - \dot{\omega}_{ni}^2(t) / \omega_{ni}^2(t) \end{cases} \tag{24}$$

Usually ζ_i is chosen as $\zeta_i = 1$ for simplification, then the only parameter to be designed is the observer bandwidth $\omega_{ni}(t)$. This is quite similar to the parameterization method in linear

ESO [8], while the difference lies in that the bandwidth here is time-varying. This time-varying mechanism offers a vast opportunity to flexibly design an observer according to specific characteristics of the observed system. Particularly, for hypersonic vehicle, during the transition from cruise to entry flight, the initial transition condition may undergo large dispersion, which means the estimated attitude values may be significantly unmatched with the true angles. In this case, if the observer gains are chosen too large, peaking phenomenon may occur and it may result in observer chattering and large power consumption. However, if the observer gains are fixed small, estimation performance may be degraded at latter stage. For this problem, we design the observer bandwidth as

$$\omega_{ni}(t) = \omega_{0i}\omega_i(t) \tag{25}$$

where ω_{0i} is a constant "nominal" bandwidth, and $\omega_i(t)$ is a time-varying multiplier. Here we design a time profile as

$$\omega_{ic}(t) = \begin{cases} a_i, & 0 < a_i < 1,\ t \le T_i \\ 1, & t > T_i \end{cases} \tag{26}$$

with adequate parameters a_i and T_i. Then $\omega_i(t)$ and its derivatives are generated by a Butterworth filter with $\omega_{ic}(t)$ as the filter input:

$$\dddot{\omega}_i(t) + 2\omega_{Bi}\ddot{\omega}_i(t) + 2\omega_{Bi}^2\dot{\omega}_i(t) + \omega_{Bi}^3\omega_i(t) = \omega_{Bi}^3\omega_{ic}(t) \tag{27}$$

with ω_{Bi} as a constant parameter for this filter. The time-varying logic (25)-(27) tells that the observer bandwidth $\omega_{ni}(t)$ grows from $a_i\omega_{0i}$ to ω_{0i}. Therefore, it can suppress peaking with a small bandwidth at the beginning and perform good estimation ability with a large bandwidth at latter stage.

Once the total disturbance Δ_s is well estimated as Z_2 (denoted as $\hat{\Delta}_s$ for better understanding) by the TESO (21) with time-varying gains (24) under the logic (25)-(27), a compensation law is integrated into the basic law (19) as

$$X_{2c}' = G_1^{-1}(X_1)[-K_1E_1 + \dot{X}_{1c} - F_1(X_1) - \hat{\Delta}_s] \tag{28}$$

At last, TESO for the fast-state loop is similarly designed. It is omitted here for page limitation.

C. Time-varying tracking differentiator design

Hypersonic entry flight features super maneuvers with diverse command shapes. In order to reduce vehicle velocity rapidly, reference command of angle of attack is often set large. Simultaneously, the vehicle descends by controlling bank angle, thus reference command of the bank angle often varies with different variation speed. However, due to constrained actuator torques, the vehicle performs quite different tracking abilities with respect to different forms of commands. For example, the vehicle may track a smooth command (such as sine-wave command) well but may fail for an abrupt command (such as step or square-wave command). Thus inappropriate command may result in tracking oscillation and actuator saturation. Moreover, significant coupling exists among aerodynamics, propulsion, and control. Thus degraded tracking in one channel may significantly affect control performance of the overall system.

This problem can be well solved by TD. By arranging a proper transient process for a given reference command according to system tracking ability, TD solves the conflict between fast response and tracking overshoot. Conventional TD adopts a nonlinear function with a parameter called "speed factor" to determine the arranged transient time. Although it performs quite well, this nonlinear TD has two drawbacks. For one thing, similarly to nonlinear ESO, theoretical derivation is difficult to be carried out for nonlinear TD. For another, as the speed factor is a pre-designed constant, the transient time cannot be flexibly adjusted according to command forms or shapes. In this paper, we propose the following linear time-varying TD as a command shaping filter for the slow-state loop:

$$\begin{cases} \dot{\eta}_{1i} = \eta_{2i} \\ \dot{\eta}_{2i} = -a_{1i}(t)(\eta_{1i} - \eta_{ic}) - a_{2i}(t)\eta_{2i} \end{cases}, i = \alpha, \beta, \mu \tag{29}$$

where η_{ic}, η_{1i}, η_{2i} are the original command, the filtered command and its derivative, i.e., $[\eta_{\alpha c}, \eta_{\beta c}, \eta_{\mu c}]^T = X_{1c}'$, $[\eta_{1\alpha}, \eta_{1\beta}, \eta_{1\mu}]^T = X_{1c}$, $[\eta_{2\alpha}, \eta_{2\beta}, \eta_{2\mu}]^T = \dot{X}_{1c}$. The time-varying gains $a_{1i}(t)$ and $a_{2i}(t)$ are set as

$$\begin{cases} a_{1i}(t) = \omega_{\eta i}^2(t) \\ a_{2i}(t) = 2\zeta_{\eta i}\omega_{\eta i}(t) - \dot{\omega}_{\eta i}(t)/\omega_{\eta i}(t) \end{cases} \tag{30}$$

where $\omega_{\eta i}(t)$ is time-varying bandwidth and $\zeta_{\eta i}$ is constant damping ratio for this shaping filter. Choose $\zeta_{\eta i} = 1$ for simplification, then $\omega_{\eta i}(t)$ is the only parameter to be tuned. Note that if $\omega_{\eta i}(t)$ is also chosen constant, (29)-(30) coincide with commonly used second-order linear filter. To adaptively adjust the filter feature, we design a time-varying logic for the filter bandwidth as

$$\omega_{\eta ic}(t) = \omega_{\eta i\_\min} + m_i\left[\text{sat}\left(\left|\dot{\eta}_{2i}\right|\right) - n_i\right] \tag{31}$$

where $\omega_{\eta ic}(t)$ is the bandwidth command, thus $\omega_{\eta i}(t)$ and $\dot{\omega}_{\eta i}(t)$ are generated by passing $\omega_{\eta ic}(t)$ through a second-order Butterworth filter. $\omega_{\eta i\_\min}$ is the minimal value of $\omega_{\eta ic}(t)$. By properly selecting constant parameters m_i, n_i, the time-varying logic (31) tells that the shaping filter bandwidth can be adaptively adjusted according to the speed of the arranged transient process: it will decrease if the process is too fast and increase if the process is too slow. Thus either abrupt or smooth commands can be well arranged and tracked.

TTD for the fast-state loop can be similarly designed and it is omitted also because of page limitation.

IV. Simulation Results

In this section, two cases are simulated. In the first case, uncertainties are not involved, while a square wave and a sine wave reference command for the bank angle with the same period and amplitude are compared, which exhibits great advantage of TTD over conventional command filter with a constant bandwidth. In the second case, besides the TTD, uncertainties and initial condition dispersion are considered, which exhibits the effectiveness of TESO in disturbance rejection and peaking suppression.

The initial GHV trimmed condition is $\alpha = 1.7533\,\text{deg}$, $\beta = \mu = 0$, $p = q = r = 0$. In the first simulation, the reference angle of attack command is given as $\eta_{\alpha c} = 8\,\text{deg}$, indicating a

large angle of attack for fast velocity reduction. The commanded sideslip angle $\eta_{\beta c}$ is always zero. For comparison, the commanded bank angle is separately set as a square wave $\eta_{\mu c} = 50\text{sign}(\sin(0.05\pi t))$ deg and a sine wave $\eta_{\mu c} = 50\sin(0.05\pi t)$ deg with the same period 40 sec and the same amplitude 50 deg. These commands simulate the bank reversal maneuver during fast reentry flight. We design a conventional bank angle command filter for comparison, i.e., the filter bandwidth $\omega_{\eta i}(t)$ in (30) is constant (denoted as $\bar{\omega}_{\eta i}$). Set $\bar{\omega}_{\eta\alpha} = 2$, $\bar{\omega}_{\eta\beta} = 1$. For the square command, the control system works well with $\bar{\omega}_{\eta\mu} = 0.5$, but actuator saturation occurs and the coupled angle of attack cannot track its reference command when $\bar{\omega}_{\eta\mu}$ is increased to 2 (see Fig. 2). The actuators experience no saturation at latter flight stage because as the vehicle descends the vehicle control ability increases as dynamic pressure increases. Continuously increase $\bar{\omega}_{\eta\mu}$ to $\bar{\omega}_{\eta\mu} = 5$, the overall system crashes. On the contrary, for the sine command, the system performs well for both $\bar{\omega}_{\eta\mu} = 2$ and $\bar{\omega}_{\eta\mu} = 5$, with fast tracking and no actuator saturation. However, $\bar{\omega}_{\eta\mu} = 0.5$ makes the filtered command undesired distortion with about 40 deg phase lag and 5 deg amplitude attenuation (see Fig. 3). This comparison indicates an obvious result that GHV can track a smooth command much better than an abrupt command.

For improvement, we design a TTD for the bank command with its minimum bandwidth $\omega_{\eta\mu}(t) = \omega_{\eta\mu\_\min} = 0.5$ and maximum $\omega_{\eta\mu}(t) = 5$. For both square and sine commands, the control system works well with fast tracking but no actuator saturation for square command or command distortion for sine command (Fig. 4). The time-varying bandwidth is depicted in Fig. 5. Particularly note that, in the square response, although at most time $\omega_{\eta\mu}(t) > 2$, it is verified that energy consumption is reduced to 44% of that with constant bandwidth $\bar{\omega}_{\eta\mu} = 2$.

In the second simulation, the TTD designed above is adopted. To verify the disturbance rejection and peaking suppression ability of TESO, a constant disturbance $\Delta_4 = 12\,\text{deg/sec}^2$ is considered for demonstration. In addition, an initial reentry dispersion exists in the roll rate, i.e., $p(0) = 0 \neq \hat{p}(0) = 5\,\text{deg/sec}$, where $p(0)$ and $\hat{p}(0)$ are the true and estimated values of the initial roll rate. Parameters for the time-varying TESO bandwidth logic (25)-(27) are selected as $\omega_{0p} = 6$, $a_p = 1/3$, $T_p = 0.5$, $\omega_{Bp} = 5$. That means the TESO bandwidth is set as small as $\omega_{np}(t) = a_p\omega_{0p} = 2$ before 0.5 sec, and then increased to $\omega_{np}(t) = \omega_{0p} = 6$. Still set original reference attitude angle commands as $\eta_{\alpha c} = 8\,\text{deg}$, $\eta_{\beta c} = 0$, $\eta_{\mu c} = 50\text{sign}(\sin(0.05\pi t))$ deg. Bank angle tracking with and without TESO is depicted in Fig. 6. There exists about 2 deg steady tracking error if no TESO added due to disturbance Δ_4. However, it performs very well if TESO added, where the estimated value is also plotted in Fig. 6. Finally, this TESO is compared with ESO using fixed bandwidth (denoted as $\bar{\omega}_{np}$). Two fixed bandwidths are considered: a large $\bar{\omega}_{np} = 6$ and a small $\bar{\omega}_{np} = 2$. In Fig. 7, it is seen that a large fixed bandwidth causes large peaking of disturbance estimation, while a small fixed bandwidth yields slow estimation. TESO with time-varying bandwidth can solve both problems. Its bandwidth is shown in Fig. 8.

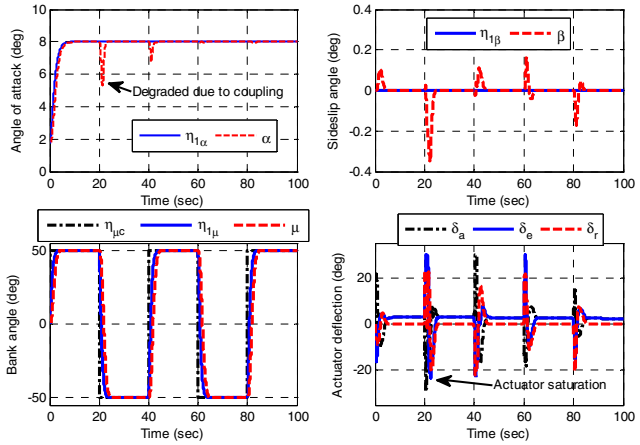

Fig.2 Square bank angle response ($\bar{\omega}_{\eta\mu} = 2$).

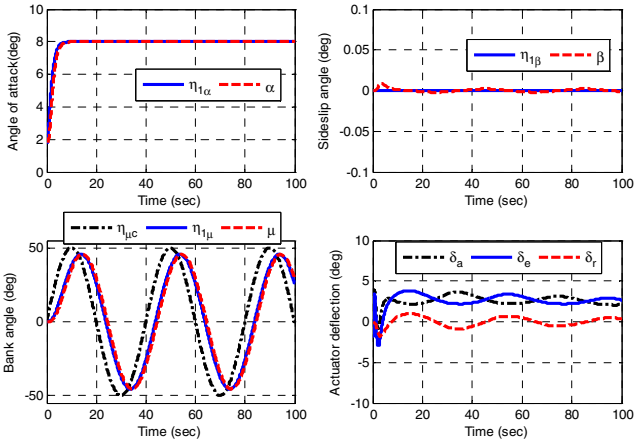

Fig.3 Sine bank angle response ($\bar{\omega}_{\eta\mu} = 0.5$).

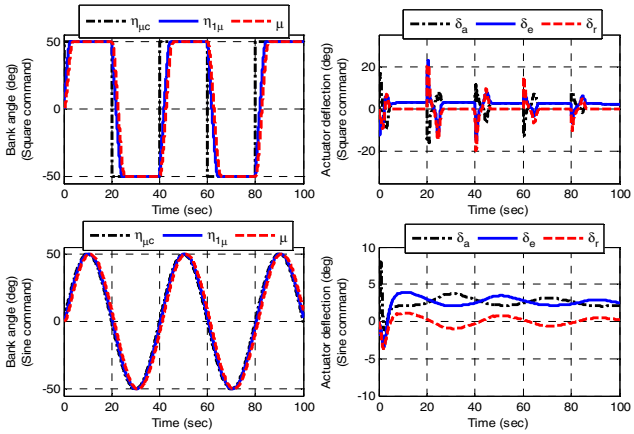

Fig.4 Square and sine bank angle responses (TTD).

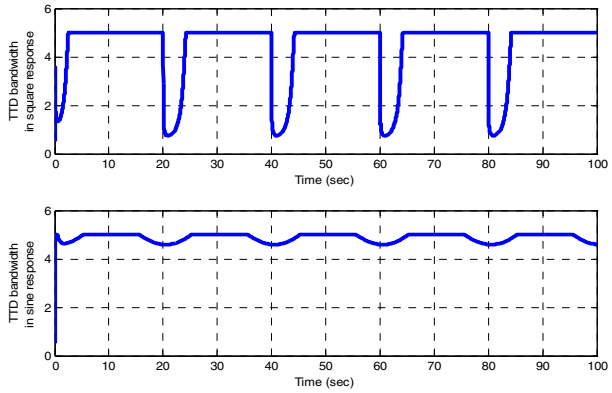

Fig.5 Time-varying bandwidth of TTD in square and sine responses.

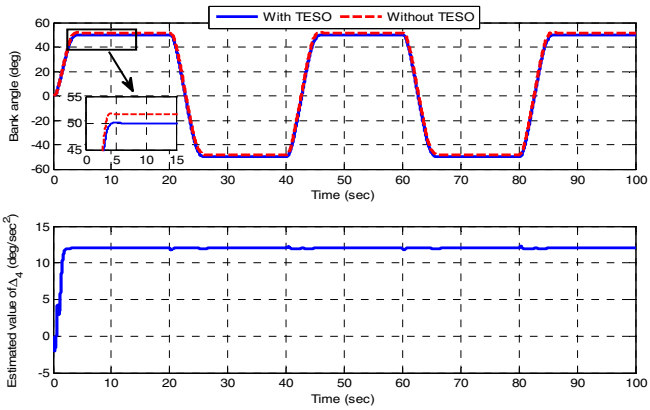

Fig.6 Bank angle tracking with and without TESO.

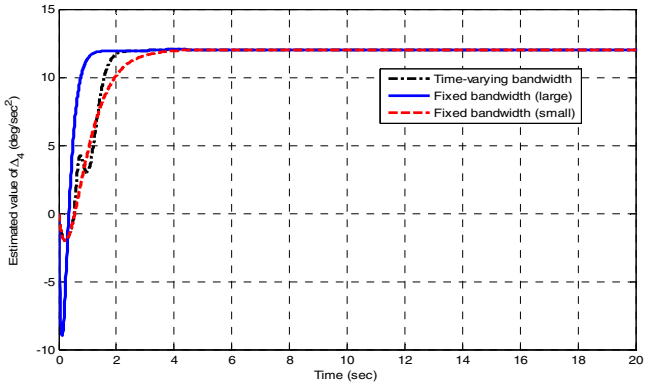

Fig.7 Estimation with time-varying and fixed bandwidths.

V. Conclusions

In this paper, an attitude control strategy for hypersonic reentry vehicle is proposed. It combines a basic dynamic inversion controller with enhanced ADRC using time-varying spectrum theory. TTD can adjust its bandwidth according to change rate of the arranged command process, thus either smooth or abrupt command can be well tracked with constrained control torques. TESO observer can also adjust its bandwidth to flexibly improve the estimation performance and, particularly, suppress peaking resulting from initial entry condition dispersion. It is seen that design of either TTD or TESO is finally simplified to design a proper time-varying logic for corresponding bandwidth. This parameterization approach leads a simple tuning method. As exemplified by the two simulations, the proposed strategy shows good attitude tracking and great design flexibility properties.

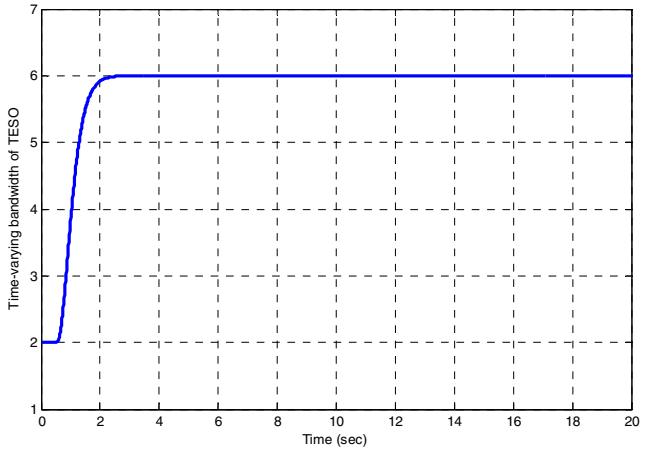

Fig.8 Time-varying bandwidth of TESO.

References

[1] H. B. Duan and S. T. Li, "Artificial bee colony-based direct collocation for reentry trajectory optimization of hypersonic vehicle," *IEEE Trans. Aero. Electron Sys.*, vol. 51, no. 1, pp. 615–626, Jan. 2015.

[2] W. R. van Soest, Q. P. Chu, and J. A. Mulder, "Combined feedback linearization and constrained model predictive control for entry flight," *J. Guid. Control Dynam.*, vol.29, no.2, pp. 427-434, Mar.-Apr. 2006.

[3] W. J. Rugh and J. S. Shamma, "Research on gain scheduling," *Automatica*, vol. 36, no. 10, pp. 1401-1425, Oct. 2000.

[4] B. Lian and H. Bang, "Adaptive backstepping control based autopilot design for reentry vehicle," in *Proc. AIAA Guid. Nav. Control Conf. Exhibit*, Rhode Island, 2004, AIAA 2004-5328.

[5] Z. Q. Pu, X. M. Tan, G. L. Fan, and J. Q. Yi, "Uncertainty analysis and robust trajectory linearization control of a flexible air-breathing hypersonic vehicle," *Acta Astronaut.*, vol.101, pp. 16-32, Jan. 2014.

[6] X. L. Shao, and H. L. Wang, "Active disturbance rejection based trajectory linearization control for hypersonic reentry vehicle with bounded uncertainties," *ISA Trans.*, vol.54, pp. 27-38, Jan. 2015.

[7] J. Han, "From PID to active disturbance rejection control," *IEEE Trans. Ind. Electron.*, vol. 56, no. 3, pp. 900-906, Mar. 2009.

[8] D. Yoo, S. Yau, and Z. Q. Gao, "Optimal fast tracking observer bandwidth of the linear extended state observer," *Internat. J. Control*, vol. 80, no. 1, pp. 102-111, Jan. 2007.

[9] Z. Q. Pu, R. Y. Yuan, J. Q. Yi, and X. M. Tan, "A class of adaptive extended state observers for nonlinear disturbed systems," *IEEE Trans. Ind. Electron.*, vol. 62, no. 9, pp. 5858-5869, Sep. 2015.

[10] J. Yao, Z. Jiao, and D. Ma, "Adaptive robust control of DC motors with extended state observer," *IEEE Trans. Ind. Electron.*, vol. 61, no. 7, pp. 3630-3637, Jul. 2014.

[11] S. Keshmiri, R. Colgren, and M. Mirmirani, "Development of an aerodynamic database for a generic hypersonic air vehicle," in *Proc. AIAA Guid., Nav., Control Conf. Exhibit*, San Francisco, 2005, AIAA 2005-6257.

[12] Z. Q. Pu, X. M. Tan, G. L. Fan and J. Q. Yi. "Design of entry trajectory tracking law for suborbital hypersonic vehicle via inversion control," In *Proc. 10th World Congress Intell. Control Automat.*, Beijing, 2012, pp. 1092-1097.